Design and Synthesis of 5-Aryl-pyridone-carboxamides as Inhibitors of Anaplastic Lymphoma Kinase

Rongshi Li,*,[†] Liquan Xue,[‡] Tong Zhu,[†] Qin Jiang,[‡] Xiaoli Cui,[‡] Zheng Yan,[†] Danny McGee,[†] Jian Wang,[†] Vidyasagar Reddy Gantla,[†] Jason C. Pickens,[†] Doug McGrath,[†] Alexander Chucholowski,[†] Stephan W. Morris,*,[‡] and Thomas R. Webb*,[†,||]

ChemBridge Research Laboratories and ChemBridge Corporation, 16981 Via Tazon, Suites K and G, San Diego, California 92127, and Departments of Pathology and Hematology-Oncology, St. Jude Children's Research Hospital, 332 N. Lauderdale Street, Memphis, Tennessee 38105

Received August 18, 2005

Anaplastic lymphoma kinase (ALK) is a promising new target for therapy of certain cancers such as anaplastic large-cell lymphoma (ALCL) and inflammatory myofibroblastic tumor (IMT). We have identified a series of novel pyridones as kinase inhibitors of ALK by application of a stepwise process involving in vitro screening of a novel targeted library followed by iterative template modification based on medicinal chemistry insights and computational ranking of virtual libraries. Using this process, we discovered ALK-selective inhibitors with improved potency and selectivity. Herein the details of the design process and synthesis of these novel pyridones, along with their enzymatic and cell-based activity, are discussed.

Introduction

Anaplastic lymphoma kinase (ALK) was originally identified by virtue of its involvement in the t(2;5)(p23;q35) chromosomal translocation that occurs in a subset of non-Hodgkin's lymphoma (NHL) known as the anaplastic large-cell lymphomas (ALCLs). In 1994, the molecular oncology research group led by Dr. Stephan W. Morris at St. Jude Children's Research Hospital published the positional cloning of the t(2;5) chromosomal rearrangement, identifying the nucleophosmin (*NPM*)−anaplastic lymphoma kinase fusion gene.[1] The normal *ALK* gene encodes a receptor tyrosine kinase (RTK) that is a member of the insulin receptor superfamily, is most highly related to leukocyte tyrosine kinase (LTK), and is expressed normally in the central and peripheral nervous systems.[2−8] The normal functions of ALK are not yet completely clear, but Alk knockout mice possess no apparent abnormalities and have a normal lifespan.[4]

The capacity of certain small molecules to selectively inhibit tyrosine kinases by competing for ATP binding at their kinase catalytic sites is now well-documented.[9−14] Such compounds are now clinically used to inhibit ABL, PDGFR, KIT, and the EGFR among other kinases, often with dramatic therapeutic benefit and minimal toxicities.[15−18] Although other approaches could theoretically be used to inhibit ALK signaling (e.g., antisense ribonucleotides, ribozymes, small interfering RNAs, receptor- or ligand-competitive antibodies, intrabodies, or agents directed against SH2/SH3-containing ALK substrates),[19−23] each has practical limitations compared to ATP-competitive small molecules. For example, antibodies interfering with ligand-mediated activation would inhibit signaling only by full-length

ALK, not the ALK fusions, such as NPM−ALK and others, that cause NHL and IMT.[4] Agents directed against molecules in ALK signaling pathways, such as STAT3, may suffer from a lack of specificity and could thus be associated with limiting toxicities.[23c] Independent of the potential therapeutic benefits of a selective and potent ALK ATP-competitive inhibitor, such a compound would also greatly facilitate the basic research analysis of ALK signaling and function because of the ability to create an inducible and reversible "pharmacological knockout" of the kinase.

Targeted therapies that are both more effective and less toxic than those currently available would be extremely valuable in the clinical management of ALK fusion-positive lymphomas and IMTs, and for the treatment of those solid tumors in which autocrine and/or paracrine stimulation of the nonmutated, wild-type ALK receptor by its ligands, pleiotrophin (PTN) and midkine (MK), is believed to occur, such as glioblastomas and others.[4,23d−23h] The recent success of the inhibitor STI571 (Gleevec, Novartis Pharmaceuticals, East Hanover, NJ), which targets the ABL, KIT, and PDGFR tyrosine kinases in the treatment of BCR-ABL-positive leukemias and KIT-positive gastrointestinal stromal tumors (GISTs) and other malignancies, has provided compelling proof-of-principle for the use of small molecule kinase inhibitors as therapeutic agents. An analogous approach has a very high likelihood of success for the treatment of ALCLs, IMTs, and solid tumors induced by ALK deregulation.

Only a few inhibitors with activity against ALK have been reported, as shown in Chart 1.[24−27] UCN-01 (**1**), a derivative of the natural product staurosporine, was reported to have antitumor activity in a patient with an ALK-positive anaplastic large cell lymphoma that was refractory to conventional chemo- and radiotherapy.[24] It is important to note that the ability of **1** to inhibit ALK was not tested in this study; thus, it has not been formally proven that **1** is an ALK inhibitor. Indeed, a recent report suggests that **1** possesses minimal ability to directly inhibit ALK.[28] The naturally occurring, structurally related benzo-quinone analogues, geldanamycin, and 17-allylamino-17-
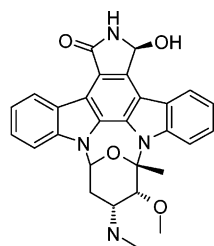
* To whom correspondence should be addressed. For R.L.: Phone (858) 485-9900. Fax (858) 485-9922. E-mail: Rongshi.li@chembridgeresearch.com. For S. W. M.: phone (901) 495-3616. Fax (901) 495−2032. E-mail: steve.morris@stjude.org.
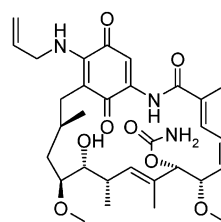† ChemBridge Research Laboratories.
|| ChemBridge Corporation.
‡ Departments of Pathology and Hematology-Oncology, St. Jude Children's Research Hospital.
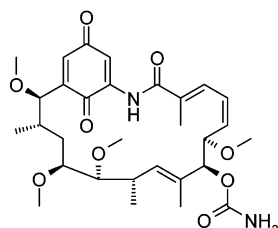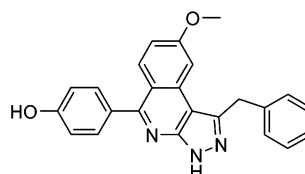
Chart 1

(1): UCN-01, 7-hydroxystaurosporine

(2): 17-allylamino,17-demethoxygeldanamycin

(3): Herbimycin A

(4): pyrazolo[3,4-c]isoquinoline

demethoxygeldanamycin[25] (**2**) and herbimycin A[26] (**3**) have been reported to exert ALK inhibition via heat shock protein pathways, enhancing the proteasome-mediated degradation of the ALK protein. Most recently, a series of pyrazolo[3,4-c]-isoquinoline derivatives (**4**) with ALK-inhibitory activity was published in a patent application.[27]

In this work, we report the identification of a series of novel pyridones as kinase inhibitors of ALK by a stepwise process involving the in vitro kinase screening of a targeted compound library that was selected from a highly diverse drug-like discovery library (the ChemBridge PHARMACophore library) by a unique pharmacophore query method. The hits derived from this screening approach were then subjected to several rounds of iterative template modification based on medicinal chemistry insights. Proposals for improving the templates were then subjected to computational ranking by docking based on ALK homology models. Using this process, we were able to develop ALK-selective inhibitors with improved potency and selectivity.

Hit to Early Lead Discovery: Design and Selection of a Kinase-Targeted Library. There are an estimated 518 kinases, constituting ca.1.7% of the human genome, in this largest enzyme family, all of which have highly conserved catalytic domains.[29] It has been well established that a spectrum of diseases, including cancer, rheumatoid arthritis, and diabetes, are modulated by kinase signaling. In this regard, the search for selective kinase inhibitors has become an important goal for researchers. Because no crystal structures of ALK are available, we chose to focus on a pharmacophore- and ligand-based approach first in our ALK inhibitor research program by screening a kinase-targeted library, which had previously been reported in abstract form.[30]

Recently, pharmacophore methods have been increasingly used as tools in the development of kinase inhibitor lead structures.[31−33] We developed a conceptually novel approach to the design of a general kinase-targeted library, with the goal of designing a library that would be applicable to any member of this large enzyme family. We realized that conceptually it should be possible to either select compounds that meet, or to exclude compounds that do not meet, two specific computationally verifiable characteristics: first, that each desired compound should have a minimal set of binding determinates (i.e., one possible pharmacophore type) that is presented by the

ligand (ATP in this case) and, second, that each desired compound should have additional diverse binding determinates that would allow for additional unique interactions that could confer selectivity. Our application of this concept relied on a pharmacophore query method for selecting compounds that exhibit the interaction types of a combination of the low-energy conformations of the adenosine portions of ATP combined with other diverse pharmacophores.[30] This query was created with a modified version of Chem-X software using three-point pharmacophores with interaction features that include hydrogen bond donors, hydrogen bond acceptors, positive charge centers, aromatic rings, or hydrophobic centers. First, a database of the low-energy pharmacophores of 5′-*O*-methyladenosine was prepared in Chem-X.[34] This 'dummy' molecule was used to mimic all low-energy interactions expressed by the adenosine portion of ATP. The triphosphate interactions were excluded since inspection of numerous published ATP active-site kinase domains cocrystallized with inhibitors did not show occupancy of the phosphate-binding region.[33] These database of three-point pharmacophores represents the likely set of possible nonphosphate interactions presented by ATP in any ATP-recognition site. Thus, compounds that do not contain significant numbers of these interaction types are unlikely to interact with any ATP-recognition site. This set of pharmacophores was then used to search a Chem-X database. During the search process, the query overlap criteria were set such that half of the query pharmacophores should be present in any computational 'hits'. The other half of the pharmacophores in the hit molecules were allowed to have 'diverse' pharmacophores, depending on the diversity of the target database. This combination of criteria allows for the selection of compounds theoretically with the potential for selectivity among the plethora of ATP-binding sites observed in nature.

To validate that this query is both effective and specific, it was used to search a Chem-X database of known kinase inhibitors, and this search scored 85% of these inhibitor compounds as 'hits' using the query. Using the same query, against a ∼70 000-compound control diverse Chem-X pharmacophore database, less than 5% of the compounds scored as 'hits'. This exercise showed that the query is both effective at finding active kinase inhibitors and specific in that only a small percentage of randomly selected compounds scored as hits. The same query method was then applied to a drug-like subset of

Chart 2

Original hits from screening
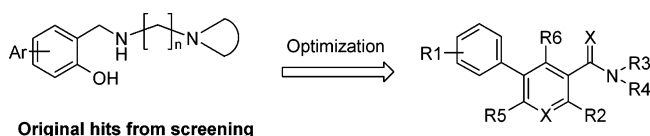
our combinatorial library based on >60 novel drug-like scaffolds (the ChemBridge PHARMACophore library; 60 000 compounds) using an even higher overlap stringency, to give a set of 2677 compounds.

In Vitro Screening and Follow-Up Library Design. As the primary screen, we have developed a high-throughput enzymatic assay to examine ALK activity, modified from the AlphaScreen (amplified luminescent proximity homogeneous assay). We have adapted this methodology to assess NPM−ALK activity based on the ability of the constitutively active purified fusion kinase to phosphorylate a biotinylated poly(GT) substrate peptide. Our high-throughput kinase enzyme inhibitor assay is best used as a primary screening tool in conjunction with more robust but lower-throughput screens, i.e., cell-based screens. Inclusion of these assays in our inhibitor screening studies addresses the possible shortcomings of our high-throughput screen; these limitations include various potential artifacts that could lead to false-positive inhibitor hits and the inability of the high-throughput screen to address the important issue of cell-based activity. This cell-based assay was initially used as a secondary screen on the hits obtained from our ALK AlphaScreen enzyme inhibitory assay to quickly determine cellular activity and selectivity of compounds. The 2677 compounds were assayed using both biochemical and cell-based screens to determine their ALK-inhibitory capabilities (see descriptions of assays in Experimental Section). Numerous 'hits' were found from several distinct structural series that showed IC$_{50}$s $\leq$ 20 μM in the biochemical ALK inhibition assay, and several compound classes were considered for follow-up. Lead optimization was performed from one of the original hits (Chart 2) that had an IC$_{50}$ in the 5 μM range, which was picked for optimization in part from computational ranking studies (vide infra) that predicted the likelihood that analogues of the hit would possess ALK-inhibitory capabilities. Consideration of the following factors and rationale was included in our optimization strategy as shown in Chart 2: (i) incorporation of an additional nitrogen atom in the center ring to acquire additional potential H-bonding interactions; (ii) increase of the rigidity of the molecule in the center ring system; (iii) selection of pharmacophoric groups from known kinase inhibitors to enhance the chances of obtaining the desired activity and selectivity; (iv) identification of appropriate spacers to link the core with the basic moiety; and (v) last, creation of a novel scaffold for patentability. A focused library of 724 virtual compounds was designed around the resulting 5-aryl-pyridone-3-carboxamide scaffold, taking into consideration novelty and Lipinski's Rule of Five.[35]

Computational Ranking of Virtual Libraries Based on in Vitro Screening Hits. a. Template Selection and Method of Building Homology Model. Structure-based drug design methods were used in our evaluation for novel scaffolds. We selected two templates in our homology modeling. The first was the insulin receptor tyrosine kinase (IRK) domain (PDB entry code: 1IR3)[36] because IRK is highly homologous to the ALK kinase domain in terms of sequence identity (45%). The crystal structure of 1IR3 is the active form of the kinase, but the shapes of our compounds of interest are more like STI571, which binds preferentially to the inactive form of the c-ABL structure, so we selected the corresponding c-ABL crystal structure (PDB

**Table 1.** Docking Results of the Pyridone and a Reference (CB1k) Libraries with the ALK Kinase Domain

library	number of compounds	number of hits	hit rate, %
CB1k	1070	14	1.3
pyridone	724	40	5.5

code: 1IEP) as our second template. The sequence identity within the kinase domains is 40% between ALK and c-ABL. To build homology models using ICM-pro, we then aligned the ALK sequence to those of the templates described above. After mapping the tentative backbone deformation zones, we predicted side chains, loops, and termini using the ICM global energy optimization. The default parameters were used in the homology modeling.[37]

b. Docking Method and Scoring Functions for Docked Structures. ICM-pro performs flexible ligand docking using an energy function including the internal energy of the ligand based on the ECEPP/3 force field, van der Waals, hydrogen-bonding, electrostatic, and hydrophobic ligand/receptor interaction terms.[38−41] The search algorithm is based on Monte Carlo Minimization (MCM) in an internal coordinate space.[40] Each step of the algorithm consists of a random conformational change of two types, torsional or positional, followed by the local minimization. Torsional movement involves complete randomization of a single arbitrarily chosen torsion angle. A positional move involves a pseudo-Brownian random translation and rotation of the ligand as a whole.[40] ICM uses an analytical gradient minimizer, which finds the local minima of the energy function more rapidly than the simplex minimizer or a stochastic search alone. To improve convergence, multiple MC runs from several starting positions are performed. The scoring function used in ICM for docked structures consists of the internal force-field energy of the ligand and the ligand/receptor interaction energy. The latter includes van der Waals terms, a hydrophobicity term based on the solvent accessible surface buried upon binding, an electrostatic solvation term (calculated using a boundary-element solution of the Poisson equation), hydrogen-bond interaction terms and an entropic term proportional to the number of flexible torsions in the ligand.[41] In our study, the docking and scoring were run three times, the best scored ligand with good contact with the ligand binding pocket (via visual inspection) was retained. Therefore, only one binding mode per ligand is considered in the current study. A docking score of less than −32 kcal/mol was defined as the hit threshold. The selection of this threshold is arbitrary; however, a study from Schapira et al. indicates that this selection is reasonable.[42] Default parameters were used throughout the docking and scoring processes.

c. Reference Library. To identify those scaffolds most likely to be potential hits for the ALK kinase, we compared the docking results from a virtual library around a scaffold of interest with those from reference compound libraries. The reference libraries (CB1k) were randomly selected from our ChemBridge historical collection with limits on the molecular property distribution characteristics on properties such as molecular weight, number of rotatable bonds, the number of nitrogen atoms and oxygen atoms, ClogP, polar surface area, and other properties, all being similar to the virtual library. The purpose of building more than one reference library is to improve the validity of the statistics obtained in the comparison.

The docking results of the pyridone library, together with our reference compound set (CB1k), against ALK are listed in Table 1. The pyridone virtual library yielded a 5.5% hit rate,

Scheme 1. Solid-Phase Synthesis of Pyridone Focused Library[a]
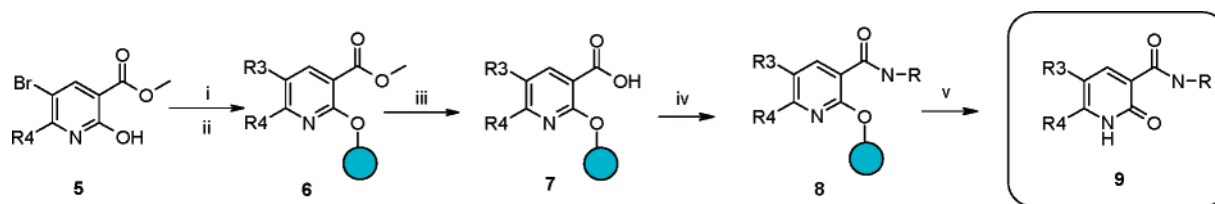
[a] Reagents and conditions: i. Wang resin, PPh$_3$, DEAD, THF; ii. R3B(OH)$_2$, Pd(PPh$_3$)$_4$, Na$_2$CO$_3$, toluene/water (3/1, v/v), 80 °C; iii. aq. NaOH (1M), THF, 50 °C; iv. RNH$_2$, HATU, DIEA, DMF; v. TFA/DCM (10%), 2 h.

while the average hit rate of the randomly selected reference library was only 1.3% with a standard deviation of 1.0%. Thus, the pyridone scaffold had an approximately four times greater likelihood to hit as a potential ALK ligand than a randomly selected compound. Therefore, pyridones may be considered a privileged scaffold for ALK based on these virtual screening results.

Results and Discussion

Follow-Up Library Synthesis. To explore this novel pyridone scaffold as kinase inhibitors, an initial focused library of 24 compounds, from a virtual library of 724 compounds, was carefully designed and synthesized using solid-phase chemistry, as shown in Scheme 1. This approach has the following advantages: (i) rapid access to a range of individual compounds; (ii) it provides a flexible means to introduce the desired diversity and to explore the available chemical space; (iii) it achieves the synthesis of the desired final library compounds that cannot be accessed by solution phase chemistry in the same time frame; and (iv) the chemistry that is developed can be quickly utilized to access the next generations of focused libraries. After the successful development of this solid-phase chemistry and library synthesis, several compounds were confirmed to be inhibitors of ALK with submicromolar potency in our in vitro kinase inhibition assay. The methodology and the scope of the chemistry, as well as its application for library synthesis, will be discussed in detail elsewhere.[43]

Structure−Activity Relationships of Pyridones. An improvement in both activity and selectivity was realized with compound **9c**, as shown in Table 2, versus the initial hits (Chart 2) that possessed enzymatic IC$_{50}$ values against ALK in the 5 μM range. This compound incorporates a group that is similar to a fragment found in Gleevec but with reversed amide functionality. While the ALK-inhibitory activity of **9c** was increased by only 6-fold compared with original hits, the 30-fold selectivity of this compound for ALK over the insulin receptor kinase (IRK) was a welcome surprise. In particular, modification of the pyridone scaffold at the 5-position was performed, taking into consideration both electronic effects and hydrogen bonding interactions. These changes resulted in decreased activity, although up to ca. 5-fold selectivity for ALK relative to the IRK was still present (**9e−i**).
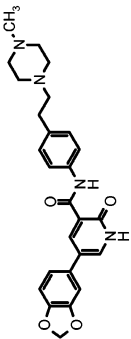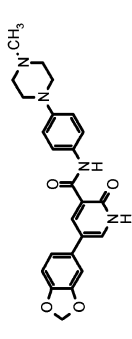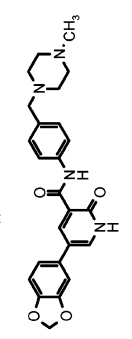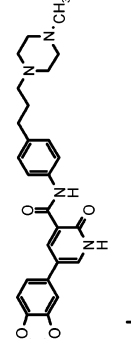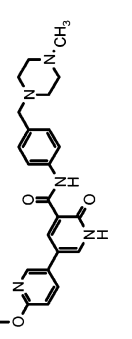
It was also discovered that an intact pyridone core is required for potent kinase inhibitory activity. First, as shown in Table 3, the inhibitory activity was reduced 4-fold by a methyl group substitution on the amide nitrogen (**9j** vs. **9c**, IC$_{50}$ of 3.7 vs 0.9 μM), presumably due to the loss of a hydrogen bond donor from amide NH of **9c**. Second, a coplanar geometric arrangement of the pyridone core with the aniline aromatic ring seems to be preferred since a l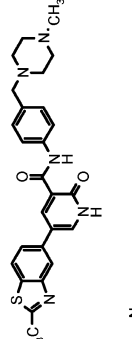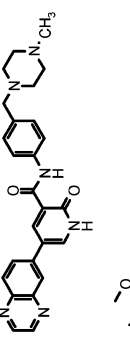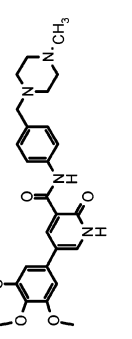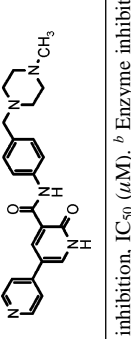oss of activity by 16-fold was observed with compounds **9k** and **9l** (~14 μM vs 0.9 μM for **9c**). Obviously,

coplanarity was disturbed by the ortho-substitution with either a methyl or methoxy group. Third, it appears that the pyridone carbonyl is acting as a hydrogen bond acceptor since a dramatic decrease in activity (20−30-folds) was observed in compounds **9m** and **9n**. The latter compounds substitute carbonyl with methoxy and chlorine, respectively (Table 3). Last, the N−H on the pyridone ring seems to be an essential hydrogen bond donor since activity was decreased by more than 50-fold when this hydrogen was replaced by a methyl group (**9o**). This observation is consistent with the proposed binding modes in the hydrogen bond donor−acceptor pharmacophore model suggested by Li and co-workers[44] and based on the general pharmacophore model for receptor tyrosine kinases.[45,46] Although the report from Li et al. was based on findings generated with the IGF1R, it is likely to be highly relevant since the "identity" and "identity and similarity" within the kinase domains of the IGF1R and ALK are 45% and 62%, respectively.

It was encouraging to observe that a set of novel pyridone derivatives showed selective inhibition of ALK compared to the IRK, as well as four other tyrosine kinases (IGF1R, Flt3, Src, Abl). As shown in Table 2, the most potent compound, **9a**, has an enzymatic ALK IC$_{50}$ of 380 nM with a K_i of 200 ± 100 nM. This compound has a 10-fold selectivity over IRK, 18-fold over IGF1R, >10-fold over Flt3, and >50-fold over both Abl and Src. The second most potent compound, **9b**, showed a similar profile to that of **9a**. Compound **9c**, with a spacer of one less carbon than **9a**, showed even higher selectivity than compound **9a** but with a 2-fold less potent ALK-inhibitory activity. Selectivity was also observed with compound **9d**, which has a longer spacer than **9a**. It was also interesting to note that all four compounds (vide supra) have activity in our cell-based antiproliferative assays, although the cellular IC50 values were in the 4−18 μM range and did not show the desired selectivity (Table 2).

A homology model of ALK built using the insulin receptor kinase domain crystal structure (PDB code: 1IR3)[36] and the c-Abl kinase domain crystal structures bound with either the small molecule inhibitors STI-571 or PD173955 (PDB codes: 1IEP and 1M52, respectively)[36,37] were employed to study the interactions between the small molecules and proteins. One of the docking results is illustrated in Figure 1. The methylenedioxyphenyl moiety and pyridone core occupy the inside pocket of the ALK kinase domain model. The H-bond donor and acceptor of the pyridone core are predicted to interact with ALK residues ASP1203 and ARG1253, espectively, as shown in Figure 2. The piperazine moiety of the molecule is exposed to solvent, which explains the observation that the activity of these analogues is not significantly sensitive to either the length of the carbon ($n = 0$−3) linker or the pattern of the substitution (Table 2).

Table 2. Kinase Inhibitory Activity of 5-Aryl-pyridone-3-carboxamide Derivatives

Entry	Structure	ALK[a]	IRK[a]	ALK[b]	IRK[b]	IGF1R[a]	Flt3[a]	Abl[a]	Src[a]	NA/BaF3[c]	BaF3[c]	Karpas299[c]	K562[c]	Jurkat[c]
9a		0.4	3.6	0.2±0.1	>20	7.0	4.0	>20	>20	17.4±3.0[d]	18.0±2.9	7.5±1.2	9.5±0.2	4.7±0.3
9b		0.7	4.8	0.6	8.8	15.0	5.0	>20	>20	6.5±2.9	6.5±2.8	3.6±1.1	3.8±1.3	3.5±0.8
9c		0.9±0.4 (n=6)	27±11 (n=6)	0.5±0.2	5.3±3.7	>20	>20	>20	>20	>25	>25	11.2±3.2	12.9±6.1	9.2±0.4
9d		1.3	10.1	1.1	9.0	>20	>20	>20	>20	13.7±5.3	16.2±5.5	9.4±0.3	14.6±5.0	9.3±0.9
9e		3.0	13.8	ND[e]	ND	ND	ND	ND	ND	ND	ND	ND	ND	ND
9f		3.8	16.0	ND	ND	ND	ND	ND	ND	ND	ND	ND	ND	ND
9g		5.5	7.0	ND	ND	ND	ND	ND	ND	ND	ND	ND	ND	ND
9h		7.5	33.5	ND	ND	ND	ND	ND	ND	ND	ND	ND	ND	ND
9i		19.5	>40	ND	ND	ND	ND	ND	ND	ND	ND	ND	ND	ND

[a] Enzyme inhibition, IC_{50} (μM). [b] Enzyme inhibition, K_i (μM). [c] Cellular antiproliferative activity, IC_{50} (μM). [d] $IC_{50} \pm SD$ (μM), $n = 3$ unless otherwise specified. [e] ND = not determined. ALK, anaplastic lymphoma kinase; IRK, insulin receptor kinase; IGF1R, insulin-like growth factor 1 receptor; Flt3, FMS-like tyrosine kinase 3; NA/BaF3; BaF3 murine lymphoid cell line engineered to express NPM−ALK; BaF3, parental interleukin-3-dependent BaF3 cell line; Karpas299, human NPM−ALK-positive anaplastic large cell lymphoma cell line; K562, human BCR-ABL-positive chronic myeloid leukemia cell line; Jurkat, human T-cell leukemia cell line. All assays were performed with two or more repetitions.

Table 3. Structure−Activity Relationship Data Concerning the Pyridone Core

Entry	Structure	ALK IC$_{50}$ (µM)	IRK IC$_{50}$ (µM)
9c		0.9±0.4 (n=6)	27±11 (n=6)
9j		3.7	32.5
9k		13.8	>40
9l		14.5	>40
9m		20.3	>40
9n		26.8	27.3
9o		>40	>40

Conclusion

5-Aryl-pyridone-3-carboxamide derivatives have been discovered as novel ALK inhibitors with IC$_{50}$s as low as 380 nM ($K_i \sim 200$ nM) and 10 to 50-fold selectivity relative to five other representative tyrosine kinases. A series of these pyridone compounds has also been shown to possess nonselective inhibitory activity of tumor cell proliferation in vitro, with cellular IC$_{50}$ values in the 4−18 µM range. Further optimization of this pyridone series is in progress to discover more potent, selective cell-penetrable compounds. Additional results will be reported in due course.

Experimental Section

All anhydrous solvents and reagents were purchased from commercial sources and used as such without further purification. The Wang resin was purchased from Polymer Labs (1.38 mmol/g). ^{1}H NMR spectra were recorded in 5 mm tubes on a 300 MHz Bruker in d_6-DMSO unless otherwise specified. Purification of compounds was performed using a Gilson HPLC system equipped with Gilson 306 pumps, Gilson 215 Liquid Handler and a Gilson UV/VIS-155 detector. Fraction collection was triggered by UV detection set within the range of 254 to 320 nm. The injection volume was 2000 µL of sample in DMSO. The mobile phase consisted of 0.1% TFA water and 0.1% TFA/acetonitrile (HPLC grade, JT Baker). Chromatographic method A was performed on an Ultra C18Q (250 × 20 mm ID, 10 µm, Peeke Scientific) column with gradients that ran from 100% to 5% aqueous for up to 43 min at a flow rate of 3 mL/min. Chromatographic method B was performed on a Kromasil C8 (250 × 20 mm ID, 10 µm) column in gradients running from 95% to 5% aqueous for up to 19 min at a flow rate of 25 mL/min.

Loading of Compound 5 (R4 = H) onto Wang Resin. To a suspension of Wang resin (10 g, Polymer Labs, 1.38 mmol/g) swollen in THF (300 mL) were added compound **5** (9.6 g, 41.4 mmol) and PPh$_3$ (10.9 g, 41.4 mmol). The resulting mixture was cooled with an ice bath, and a solution of DEAD (7.2 g, dissolved in 40 mL of THF) was added dropwise. After the addition was complete (15 min.), the reaction mixture was allowed to warm to ambient temperature gradually and stirred very gently for 18 h. The resin was collected by filtration and washed with DMF (3 × 300 mL), MeOH (3 × 300 mL), DCM (3 × 300 mL), and ether (300 mL). The resin was dried under vacuum and dispensed into

Figure 1. Predicted docking orientation of compound **9c** in ALK kinase domain homology model. Compound **9c** (space-filling); ALK kinase domain homology model (ribbon).
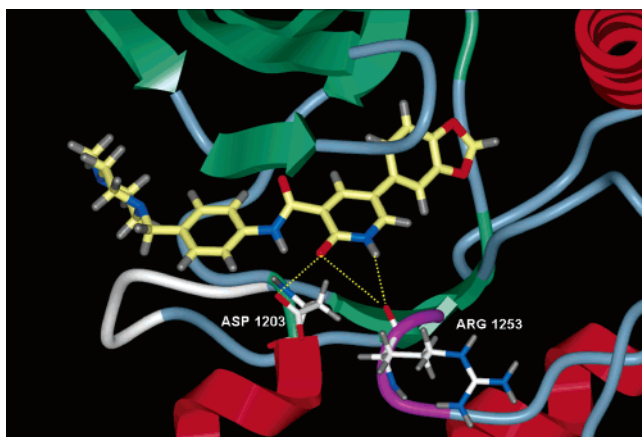
Figure 2. Putative hydrogen bonding interactions between pyridone moiety and the ALK homology model. The image shows compound **9c** within the ALK kinase domain. The hydrogen bond donor and acceptor of the pyridone core are predicted to interact with ALK residues ASP1203 and ARG1253 (numbering of the amino acids is based on the full-length ALK receptor sequence; NCBI database accession no. AAB71619).

MiniKans (75 mg each) along with an RF tag (MiniKans and RF tags were purchased from Discovery Partners International, San Diego, CA).

General Procedure for Preparation of Compound 6 (Suzuki coupling). The resin in IRORI MiniKan was swollen in toluene (3 mL for each Kan). The boronic acid (3 equiv) and aqueous Na$_2$CO$_3$ solution (1 M, 1 mL for each Kan) were added. The resulting mixture was degassed with a stream of N$_2$ for 2 min. Then, Pd(PPh$_3$)$_4$ (10%, 10 μmol for each Kan) was added and the mixture was heated at 80 °C with shaking on an orbital shaker for 18 h. The solvent was drained, and the resin was washed three times with water, DMF, DCM, MeOH, and ether successively.

General Procedure for the Preparation of Compound 8. The resin in MiniKan was swollen in THF/MeOH (1/1, v/v, 3 mL for each Kan). 1 M NaOH solution in water (0.2 mL for each Kan)

was added, and the mixture was heated at 50 °C for 12 h. 1 M HCl solution (0.2 mL for each Kan) was added, and the resin was washed three times with water, MeOH, DCM successively, and dried. The resulting resin was then swollen in DMF (3 mL for each Kan) for 30 min. After addition of the aniline (2 equiv) and DIEA (4 equiv), HATU (2 equiv) was added and the mixture was shaken overnight at room temperature. The solvent was drained, and the resin was washed three times with DMF, MeOH, and DCM successively. Finally, the resin was dried in vacuo.

General Procedure for TFA-Mediated Cleavage. The resin in a MiniKan was placed in an 8-mL vial, and 10% TFA solution in DCM (3 mL) was added. The mixture was shaken at room temperature for 2 h, and the solution was collected. The resin was washed with DCM, and the solution was combined and evaporated to dryness. The final products (**9a**−**l**) were purified by HPLC and characterized by ^{1}H NMR and LC/MS.

5-Benzo[1,3]dioxol-5-yl-2-oxo-1,2-dihydro-pyridine-3-carboxylic Acid {4-[2-(4-Methyl-piperazin-1-yl)-ethyl]-phenyl}-amide (9a). ^{1}H NMR (300 MHz, d_6-DMSO) δ 8.65 (s, 1H), 8.06 (m, 1H), 7.68 (d, 2H, J = 6 Hz), 7.28 (m, 3H), 7.11 (d, 1H, J = 6 Hz), 7.00 (d, 1H, J = 6 Hz), 3.49−3.00 (m, 10H), 2.89 (m, 2H), 2.79 (s, 3H). MS: m/z = 461.0 [M + H]$^+$. Purity: 99.5% ELSD.

5-Benzo[1,3]dioxol-5-yl-2-oxo-1,2-dihydro-pyridine-3-carboxylic Acid [4-(4-Methyl-piperazin-1-yl)-phenyl]-amide (9b). ^{1}H NMR (300 MHz, d_6-DMSO) δ 9.70 (brs, 1H), 8.64 (s, 1H), 8.05 (s, 1H), 7.63 (d, 2H, J = 9 Hz), 7.28 (s, 1H), 7.12−6.99 (m, 4H), 6.07 (s, 2H), 3.82 (m, 2H), 3.50 (m, 2H), 3.20 (m, 2H), 2.95 (m, 2H), 2.86 (s, 3H). MS: m/z = 433.0 [M + H]$^+$. Purity: 100% ELSD.

5-Benzo[1,3]dioxol-5-yl-2-oxo-1,2-dihydro-pyridine-3-carboxylic Acid [4-(4-Methyl-piperazin-1-ylmethyl)-phenyl]-amide (9c). ^{1}H NMR (300 MHz, d_6-DMSO) δ 8.65 (s, 1H), 8.05 (brs, 1H), 7.78 (d, 2H, J = 9 Hz), 7.43 (d, 2H, J = 9 Hz), 7.28 (s, 1H), 7.13 (d, 1H, J = 9 Hz), 7.02 (d, 1H, J = 9 Hz), 6.07 (s, 2H), 4.00 (m, 2H), 3.50−3.10 (m, 6H), 3.26 (m, 2H), 3.21 (s, 3H). MS: m/z = 447.0 [M + H]$^+$. Purity: 99% ELSD.

5-Benzo[1,3]dioxol-5-yl-2-oxo-1,2-dihydro-pyridine-3-carboxylic Acid {4-[3-(4-Methyl-piperazin-1-yl)-propyl]-phenyl}-amide (9d). ^{1}H NMR (300 MHz, d_6-DMSO) δ 9.89 (m, 1H), 8.54 (s, 1H), 7.97 (m, 1H), 7.23 (s, 1H), 7.07−6.97 (m, 2H), 6.06 (s, 2H), 3.54−3.00 (m, 12H), 2.73 (s, 3H), 1.80 (m, 2H). MS: m/z = 475.0 [M + H]$^+$. Purity: 100% ELSD.

6′-Methoxy-6-oxo-1,6-dihydro-[3,3′]bipyridinyl-5-carboxylic Acid [4-(4-Methyl-piperazin-1-ylmethyl)-phenyl]-amide (9e). ^{1}H NMR (300 MHz, d_6-DMSO) δ 8.68 (s, 1H), 8.45 (s, 1H), 8.17 (brs, 1H), 8.09 (d, 1H, J = 8.4 Hz), 7.77 (d, 2H, J = 8.4 Hz), 7.43 (d, 2H, J = 8.4 Hz), 6.92 (d, 1H, J = 8.4 Hz), 4.00 (brs, 2H), 3.90 (s, 3H), 3.30 (m, 8H), 2.82 (s, 3H). MS: m/z = 434.0 [M + H]$^+$. Purity: 100% ELSD.

5-(2-Methyl-benzothiazol-5-yl)-2-oxo-1,2-dihydro-pyridine-3-carboxylic Acid [4-(4-Methyl-piperazin-1-ylmethyl)-phenyl]-amide (9f). ^{1}H NMR (300 MHz, CD$_3$OD) δ 2.87 (s, 3 H), 3.04 (s, 3 H), 3.40−3.75 (brs, 8 H), 4.34 (s, 2 H), 7.58 (d, J = 8.2 Hz, 2 H), 7.66 (d, J = 8.3 Hz, 2 H), 7.87 (d, J = 8.2 Hz, 1 H), 8.04 (d, J = 8.3 Hz, 1 H), 8.09 (s, 1 H), 8.13 (s, 1 H), 8.94 (s, 1 H). MS m/z = 474.0 [M + H]$^+$. Purity: 93% ELSD.

2-Oxo-5-quinoxalin-6-yl-1,2-dihydro-pyridine-3-carboxylic Acid [4-(4-Methyl-piperazin-1-ylmethyl)-phenyl]-amide (9 g). ^{1}H NMR (300 MHz, CD$_3$OD) δ 2.85 (s, 3 H), 3.15−3.35 (brs, 8 H), 3.89 (s, 2 H), 7.35 (d, J = 9.0 Hz, 2 H), 7.66 (d, J = 9.0 Hz, 2 H), 8.06 (s, 1 H) and 8.09 (d, J = 6.0 Hz, 1 H) overlapped, 8.19 (s, 1 H) and 8.21 (d, J = 6.0 Hz, 1 H) overlapped, 8.83 (d, J = 12 Hz, 2 H), 8.95 (s, 1 H). MS m/z = 455.0 [M + H]$^+$. Purity: 96.5% ELSD.

5-(3,4,5-trimethoxyphenyl)-2-oxo-1,2-dihydro-pyridine-3-carboxylic Acid [4(4-Methylpiperazin-1-yl)methyl]phenyl-amide (9h). ^{1}H NMR (300 MHz, d_6-DMSO) δ 8.73 (s, 1H), 8.21 (brs, 1H), 7.79−7.76 (m, 2H), 7.45−7.42 (m, 2H), 7.11 (s, 2H), 4.03 (brs, 2H), 3.87 (s, 6H), 3.77 (s, 3H), 3.30 (br, 8H), 2.83 (s, 3H). MS: m/z = 493.0 [M + H]$^+$. Purity: 96.5% ELSD.

6-Oxo-1,6-dihydro-[3,4′]bipyridinyl-5-carboxylic Acid [4-(4-Methyl-piperazin-1-ylmethyl)-phenyl]-amide (9i). ^{1}H NMR (300 MHz, d_6-DMSO) δ 8.81 (d, 1H, J = 2.8 Hz), 8.62 (d, 2H, J = 8.4 Hz), 8.38 (d, 1H, J = 2.8 Hz), 7.74−7.65 (m, 4H), 7.29 (d, 2H, J = 8.4 Hz), 3.44 (s, 2H), 2.40 (m, 8H), 2.22 (s, 3H). MS: m/z = 404.0 [M + H]$^+$. Purity: 100% ELSD.

5-Benzo[1,3]dioxol-5-yl-2-oxo-1,2-dihydro-pyridine-3-carboxylic Acid Methyl-[4-(4-methyl-piperazin-1-ylmethyl)-phenyl]-amide (9j). ^{1}H NMR (300 MHz, d_6-DMSO) δ 8.66 (s, 1H), 8.08 (s, 1H), 7.79 (d, 2H, J = 6 Hz), 7.40 (d, 2H, J = 6 Hz), 7.22 (s, 1H), 7.10 (d, 1H, J = 6 Hz), 7.02 (d, 1H, J = 6 Hz), 6.07 (s, 2H), 3.94 (m, 2H), 3.53 (m, 4H), 3.17−3.08 (m, 10H). MS: m/z = 461.0 [M + H]$^+$. Purity: 97.5% ELSD.

5-Benzo[1,3]dioxol-5-yl-2-oxo-1,2-dihydro-pyridine-3-carboxylic Acid [2-Methoxy-4-(4-methyl-piperazin-1-ylmethyl)-phenyl]-amide (9k). ^{1}H NMR (300 MHz, d_6-DMSO) δ 8.66 (s, 1H), 8.53 (d, 1H, J = 9 Hz), 8.05 (m, 1H), 7.27 (s, 1H), 7.13−7.02 (m, 2H), 6.07 (s, 2H), 3.92 (m, 5H), 3.60−3.00 (m, 8H), 2.73 (s, 3H). MS: m/z = 477.0 [M + H]$^+$. Purity: 99.5% ELSD.

5-Benzo[1,3]dioxol-5-yl-2-oxo-1,2-dihydro-pyridine-3-carboxylic Acid [2-Methyl-4-(4-methyl-piperazin-1-ylmethyl)-phenyl]-amide (9l). ^{1}H NMR (300 MHz, d_6-DMSO) δ: 8.69 (s, 1H), 8.38 (d, 1H, J = 9 Hz), 8.10 (m, 1H), 7.28−7.25 (m, 4H), 7.11 (d, 1H, J = 9 Hz), 7.02 (d, 1H, J = 9 Hz), 6.07 (s, 2H), 4.09−3.38 (m, 4H), 3.43 (m, 2H), 3.16 (m, 4H), 2.80 (s, 3H), 2.36 (s, 3H). MS: m/z = 461.0 [M + H]$^+$. Purity: 100% ELSD.

5-Benzo[1,3]dioxol-5-yl-2-methoxy-*N*-[4-(4-methyl-piperazin-1-ylmethyl)-phenyl]-nicotinamide (9m). To a solution of 5-bromo-2-methoxynicotinic acid (46 mg, 200 μmol) in DMF (4 mL) was added 4-[(4-methylpiperazin-1-yl)methyl]aniline (41 mg, 200 μmol), followed by HATU (84 mg, 220 μmol) and DIEA (70 μL, 400 μmol). The mixture was stirred at room temperature for 2 h. Solvents were removed under reduced pressure, and the residue was redissolved in DCM (60 mL), which was washed with concentrated ammonia hydroxide (15 mL) and brine successively. The organic phase was concentrated, and the crude product was purified by column chromatography to give the desired amide (69 mg, 166 μmol, 83%). The bromonicotinamide (42 mg, 100 μmol) and 3,4-methylenedioxyphenyl boronic acid (33 mg, 200 μmol) were suspended in toluene (3 mL), and 1 mL of 1N solution of Na_2CO_3 was added. The suspension was degassed with a stream of N_2 for 2 min. After that, Pd(PPh$_3$)$_4$ (6 mg, 5 umol) was added and the mixture was heated at 80 °C for 18 h. The mixture was diluted with ethyl acetate (50 mL) and washed with water and brine. The organic layer was concentrated, and the residue was purified by reverse phase HPLC to give the title compound as a white solid (17 mg). ^{1}H NMR (300 MHz, d_6-DMSO) δ 10.33 (s, 1H), 8.59 (s, 1H), 8.21 (s, 1H), 7.75 (d, 2H, J = 6 Hz), 7.33 (m, 3H), 7.20 (d, 1H, J = 6 Hz), 7.03 (d, 1H, J = 6 Hz), 6.11 (s, 2H), 4.00 (s, 3H), 3.72−3.26 (m, 6H), 3.15−3.05 (m, 4H), 2.78 (s, 3H). MS: m/z = 461.0 [M + H]$^+$. Purity: 99% ELSD.

5-Benzo[1,3]dioxol-5-yl-2-chloro-*N*-[4-(4-methyl-piperazin-1-ylmethyl)-phenyl]-nicotinamide (9n). This compound was synthesized in solution phase using 5-bromo-2-chloronicotinic acid as starting material as described for the synthesis compound **9m**. ^{1}H NMR (300 MHz, CDCl$_3$) δ 2.34 (s, 3 H), 2.40−2.60 (brs, 8 H), 3.52 (s, 2 H), 6.03 (s, 2 H), 6.94 (d, J = 6.0 Hz, 1 H), 7.09 (d, J = 6.0 Hz, 1 H), 7.38 (d, J = 9.0 Hz, 2 H), 7.63 (d, J = 9.0 Hz, 2 H), 8.25 (s, 1 H), 8.30 (s, 1 H), 8.64 (s, 1 H). MS m/z = 465.0 [M + H]$^+$. Purity: 100% ELSD.

5-Benzo[1,3]dioxol-5-yl-1-methyl-2-oxo-1,2-dihydro-pyridine-3-carboxylic Acid [4-(4-Methyl-piperazin-1-ylmethyl)-phenyl]-amide (9o). This compound was synthesized in solution phase using 5-bromo-1-methyl-2-pyridone-3-carboxylic acid as starting material as described for the synthesis of compound **9m**. ^{1}H NMR (300 MHz, d_6-DMSO) δ 9.65 (s, 1H), 8.53 (s, 1H), 7.78 (d, 2H, J = 9 Hz), 7.42 (d, 2H, J = 9 Hz), 7.26 (s, 1H), 7.12 (d, 1H, J = 9 Hz), 7.03 (d, 1H, J = 9 Hz), 6.08 (s, 2H), 4.41 (m, 2H), 3.97 (m, 2H), 3.71 (s, 3H), 3.47−3.00 (m, 6H), 2.88 (s, 3H). MS: m/z = 461.0 [M + H]$^+$. Purity: 98.5% ELSD.

Enzymatic Kinase Assay for High-Throughput Screening of Candidate Small Molecule ALK Inhibitors. We developed a high-throughput enzymatic assay to examine ALK activity, modified from the AlphaScreen (Amplified Luminescent Proximity Homogeneous Assay) technology marketed by PerkinElmer Life Sciences (Boston, MA). This methodology was adapted to assess NPM−ALK activity based on the ability of the constitutively active purified fusion kinase to phosphorylate a biotinylated poly(GT) substrate peptide. NPM−ALK activity is indicated in this assay by a shift in the incident 680 nM wavelength light to an emitted wavelength between 520 and 620 nM when "donor" and "acceptor" beads come into proximity due to tyrosine phosphorylation by the purified kinase of a biotinylated-poly(GT) (G:T = 4:1) peptide bound to the streptavidin-coated "donor" bead and recognition of this phosphorylation by anti-phosphotyrosine antibody bound to the "acceptor" bead. "Donor" beads contain a photosensitizer that converts ambient oxygen to the excited singlet state when exposed to laser light at 680 nM. These singlet oxygen molecules diffuse to react with a thioxene derivative in "acceptor" beads that are in proximity to the "donor" beads (if separated by <200 nM), in turn shifting the emission wavelength to 520−620 nM. In the complete absence of NPM−ALK activity, the incident and emitted wavelengths are identical (i.e., 680 nM); partial degrees of kinase inhibition can be quantitatively scored based on the amount of wavelength shift.

A brief description of specific assay conditions follows. Compounds with a range of concentrations 40 μM, 20 μM, 10 μM, 5 μM, 2.5 μM, 1.25 μM, 0.625 μM, 0.3125 μM, 0.15625 μM, and 0.078125 μM were incubated with NPM−ALK, which was produced in insect cells as a 6xHIS-tagged fusion protein and purified using nickel-charged resin chromatography, for 30 min at RT in the presence of 10 μM ATP and 7.0 ng of biotinylated poly-GT. A 1:1 mixture of receptor and donor beads was then added to the reaction and incubated for an additional 60 min at RT. The assay was conducted on a MultiPROBE liquid handling workstation (PerkinElmer) in a 384-well plate format with a total reaction volume of 40 μL per well. Working stocks of all compounds were dissolved in 100% DMSO and serial dilutions of the compounds were performed using kinase buffer (50 mM Tris-HCl (pH 7.5), 5 mM MgCl$_2$, 5 mM MnCl$_2$, 2 mM DTT [added freshly before use], 0.01% Tween-20) containing 5% DMSO. Control samples included on all assays included kinase buffer containing 5% DMSO without compound, as well as staurosporine, which we have shown to inhibit NPM−ALK with a K_i of ∼30−50 nM. Data were collected as optical readings at 520−680 nm on a Fusion microplate analyzer (PerkinElmer), and IC$_{50}$ and K_i values calculated using PRISM3.0 software (GraphPad Software, Inc., San Diego, CA). The same assay was also used with minor modifications to assess the IC$_{50}$ and K_i values for selected compounds against five other tyrosine kinases (IRK, IGF1R, Flt3, Abl, Src), all of which were purchased from commercial vendors. Vendor information for assay reagents and materials is as follows: polyGT-Biotin: CIS Biointernational Cat. # 61GT0BLD, ATP: Sigma Cat. # A7699, sodium orthovanadate: Sigma Cat. # S-6508, Phosphotyrosine (PT66) assay kit: PerkinElmer Cat. # 6760602M, automated workstation tips (20 μL): PerkinElmer Cat. # 6000657, OptiPlate-384 (white): PerkinElmer Cat. # 6007299.

Cell-Based XTT Assay for Screening of Small Molecule Inhibitors. The IL-3-dependent lymphoid cell line BaF3 or BaF3 rendered IL-3-independent by engineered expression of NPM−ALK were used in parallel to test each candidate inhibitor. Control wells contained DMSO solvent without test compound. Specific inhibition of ALK signaling is indicated in the assay by impairment of NPM−ALK-expressing BaF3 cell growth without alterations in the growth of parental BaF3. This colorimetric assay of cell proliferation and viability is based upon reduction of the yellow monotetrazolium salt XTT to a water-soluble orange formazan dye, a reaction catalyzed by mitochondrial dehydrogenases in living cells only (Cell Proliferation Kit II, Cat. # 1 465 015, Roche Biochemicals). In addition to testing compounds for their ability to impair the growth of BaF3 cells engineered to express NPM−ALK, the NPM−ALK-positive human lymphoma cell line Karpas-

299 (Deutsche Sammlung von Mikroorganismen und Zellkulturen GmbH [DSMZ] no. ACC 31), the human BCR-ABL-positive chronic myeloid leukemia cell line K562 (American Type Culture Collection [ATCC] no. CCL-243), and the human T-cell leukemia line Jurkat (DSMZ no. ACC 282) were tested in these assays as well.

Specifics regarding the cell-based assays follow. Each compound stock in 100% DMSO was first diluted using 8% DMSO/culture medium to produce a working stock of 250 μM compound. This working stock was then used to perform serial 1:1 dilutions (i.e., 125 μM, 62.5 μM, 31.25 μM, 15.625 μM, 7.8125 μM, and 3.90625 μM) using DMSO-free culture medium. Twenty (20) microliters of each of these dilutions was then added to the cells (2 × 10^4 cells in 80 μL of culture medium per 96-well) to obtain the final test compound concentrations (i.e., 25 μM, 12.5 μM, 6.25 μM, 3.125 μM, 1.5625 μM, and 0.78125 μM). The maximum final DMSO concentration in the assays was 2.61%, which was found to have no effect on cell viability and proliferation. The assays were read and the cellular IC$_{50}$s determined 72 h following addition of the test compounds to the cultures.

Supporting Information Available: Purity of compounds **9a** through **9o** by elemental analysis and high resolution of mass spectrometry with two diverse HPLC systems is available free of charge via the Internet at http://pubs.acs.org.

References

(1) Morris, S. W.; Kirstein, M. N.; Valentine, M. B.; Dittmer, K. G.; Shapiro, D. N.; Saltman, D. L.; Look, A. T. Fusion of a kinase gene, ALK, to a nucleolar protein gene, NPM, in non-Hodgkin's lymphoma. *Science* **1994**, *263*, 1281–1284.

(2) Iwahara, T.; Fujimoto, J.; Wen, D.; Cupples, R.; Bucay, N.; Arakawa, T.; Mori, S.; Ratzkin, B.; Yamamoto, T. Molecular characterization of ALK, a receptor tyrosine kinase expressed specifically in the nervous system. *Oncogene* **1997**, *14*, 439–449.

(3) Morris, S. W.; Naeve, C.; Mathew, P.; James, P. L.; Kirstein, M. N.; Cui, X.; Witte, D. P. *ALK*, the chromosome 2 gene locus altered by the t(2; 5) in non-Hodgkin's lymphoma, encodes a neural receptor tyrosine kinase that is highly related to leukocyte tyrosine kinase (LTK). *Oncogene* **1997**, *14*, 2175–2188.

(4) Pulford, K. P.; Morris, S. W.; Turturro, F. Anaplastic lymphoma kinase proteins in growth control and cancer. *J. Cell. Physiol.* **2004**, *199*, 330–358.

(5) Bernards, A.; de la Monte, S. M. The ltk receptor tyrosine kinase is expressed in pre-B lymphocytes and cerebral neurons and uses a non-AUG translational initiator. *EMBO J.* **1990**, *9*, 2279–2287.

(6) Krolewski, J. J.; Dalla-Favera, R. The ltk gene encodes a novel receptor-type protein tyrosine kinase. *EMBO J.* **1991**, *10*, 2911–2919.

(7) Snijders, A. J.; Haase, V. H.; Bernards, A. Four tissue-specific mouse ltk mRNAs predict tyrosine kinases that differ upstream of their transmembrane segment. *Oncogene* **1993**, *8*, 27–35.

(8) Toyoshima, H.; Kozutsumi, H.; Maru, Y.; Hagiwara, K.; Furuya, A.; Mioh, H.; Hanai, N.; Takaku, F.; Yazaki, Y.; Hirai, H. Differently spliced cDNAs of human leukocyte tyrosine kinase receptor tyrosine kinase predict receptor proteins with and without a tyrosine kinase domain and a soluble receptor protein. *Proc. Natl. Acad. Sci. U.S.A.* **1993**, *90*, 5404–5408.

(9) Boschelli, D. H. Small molecule inhibitors of receptor tyrosine kinases. *Drugs Future* **1999**, *24*, 515–537.

(10) Toledo, L. M.; Lydon, N. B.; Elbaum, D. The structure-based design of ATP-site directed protein kinase inhibitors. *Curr. Med. Chem.* **1999**, *6*, 775–805.

(11) Al-Obeidi, F. A.; Lam, K. S. Development of inhibitors for protein tyrosine kinases. *Oncogene* **2000**, *19*, 5690–5701.

(12) Morin, M. J. From oncogene to drug: development of small molecule tyrosine kinase inhibitors as anti-tumor and anti-angiogenic agents. *Oncogene* **2000**, *19*, 6574–6583.

(13) Buchdunger, E.; Matter, A.; Druker, B. J. Bcr-Abl inhibition as a modality of CML therapeutics. *Biochim. Biophys. Acta* **2001**, *1551*, M11–M18.

(14) Ruggeri, B. A.; Miknyoczki, S. J.; Singh, J.; Hudkins, R. L. Role of neurotrophin-trk interactions in oncology: the antitumor efficacy of potent and selective trk tyrosine kinase inhibitors in pre-clinical tumor models. *Curr. Med. Chem.* **1999**, *6*, 845–847.

(15) Druker, B.; Lydon, N. B. Lessons learned from the development of an Abl tyrosine kinase inhibitor for chronic myelogenous leukemia. *J. Clin. Invest.* **2000**, *105*, 3–7.

(16) Druker, B. J.; Talpaz, M.; Resta, D. J.; Peng, B.; Buchdunger, E.; Ford, J. M.; Kantarjian, H.; Capdeville, R.; Ohno-Jones, S.; Sawyers, C. L. Efficacy and safety of a specific inhibitor of the Bcr-Abl tyrosine kinase in chronic myeloid leukemia. *N. Engl. J. Med.* **2001**, *344*, 1031–1037.

(17) Druker, B. J.; Sawyers; C. L.; Kantarjian, H.; Resta, D. J.; Reese, S. F.; Ford, J. M.; Talpaz, M. Activity of a specific inhibitor of the Bcr-Abl tyrosine kinase in blast crisis of chronic myeloid leukemia and acute lymphoblastic leukemia with the Philadelphia chromosome. *N. Engl. J. Med.* **2001**, *344*, 1038–1042.

(18) (a) Joensuu, H.; Roberts, P. J.; Sarlomo-Rikala, M.; Andersson, L. C.; Tuveson, D.; Silberman, S.; Capdeville, R.; Dimitrijevic, S.; Druker, B. Effect of the tyrosine kinase inhibitor STI571 in a patient with a metastatic gastrointestinal stromal tumor. *N. Engl. J. Med.* **2001**, *344*, 1052–1056. (b) Steinert, D. M.; McAuliffe, J. C.; Trent, J. C. Imatinib mesylate in the treatment of gastrointestinal stromal tumour. *Expert Opin. Pharmacother.* **2005**, *6*, 105–113. (c) Sakamoto, K. M. SU-11248 Sugen. *Curr Opin Investig Drugs* **2004**, *5*, 1329–1339. (d) Burgess, M. R.; Skaggs, B. J.; Shah, N. P.; Lee, F. Y.; Sawyers, C. L. Comparative analysis of two clinically active BCR-ABL kinase inhibitors reveals the role of conformation-specific binding in resistance. *Proc. Natl. Acad. Sci. U.S.A.* **2005**, *102*, 3395–4000. (e) Baselga, J.; Arteaga, C. L. Critical update and emerging trends in epidermal growth factor receptor targeting in cancer. *J. Clin. Oncol.* **2005**, *23*, 2445–2459.

(19) Tamm, I.; Dorken, B.; Hartmann, G. Antisense therapy in oncology: new hope for an old idea. *Lancet* **2001**, *358*, 489–497.

(20) Kuywabara, T.; Warashina, M.; Taira, K. Allosterically controllable maxizymes cleave mRNA with high efficiency and specificity. *Trends Biotechnol.* **2000**, *18*, 462–468.

(21) (a) Tanabe, T.; Kuwabara, T.; Warashina, M.; Tani, K.; Taira, K.; Asano, S. Oncogene inactivation in a mouse model. *Nature* **2000**, *406*, 473–474. (b) Song, E.; Zhu, P.; Lee, S. K.; Chowdhury, D.; Kussman, S.; Dykxhoorn, D. M.; Feng, Y.; Palliser, D.; Weiner, D. B.; Shankar, P.; Marasco, W. A.; Lieberman, J. Antibody mediated in vivo delivery of small interfering RNAs via cell-surface receptors. *Nat. Biotechnol.* **2005**, *23*, 709–717.

(22) (a) Mosesson, Y.; Yarden, Y. Oncogenic growth factor receptors: implications for signal transduction therapy. *Semin. Cancer Biol.* **2004**, *14*, 262–270. (b) Marasco, W. A.; Jones, S. D. Antibodies for targeted gene therapy: extracellular gene targeting and intracellular expression. *Adv. Drug Delivery Rev.* **1998**, *31*, 153–170.

(23) (a) Lobato, M. N.; Rabbitts, T. H. Intracellular antibodies as specific reagents for functional ablation: future therapeutic molecules. *Curr. Mol. Med.* **2004**, *4*, 519–528. (b) Gao, Y.; Luo, J.; Yao, Z. J.; Guo, R.; Zou, H.; Kelley, J.; Voigt, J. H.; Yang, D. Inhibition of Grb2 SH2 domain binding by nonphosphate-containing ligands. 2. 4-(2-Malonyl) phenylalanine as a potent phosphotyrosine mimetic. *J. Med. Chem.* **2000**, *43*, 911–920. (c) Chiarle, R.; Simmons, W. J.; Cai,. H.; Dhall, G.; Zamo, A.; Raz, R.; Karras, J. G.; Levy, D. E.; Inghirami, G. Stat3 is required for ALK-mediated lymphomagenesis and provides a possible therapeutic target. *Nat. Med.* **2005**, *11*, 623–629. (d) Stoica, G. E.; Kuo, A.; Aigner, A.; Sunitha, I.; Souttou, B.; Malerczyk, C.; Caughey, D. J.; Wen, D.; Karavanov, A.; Riegel, A. T.; Wellstein, A. Identification of anaplastic lymphoma kinase as a receptor for the growth factor pleiotrophin. *J. Biol. Chem.* **2001**, *276*, 16772–16779. (e) Bowden, E. T.; Stoica, G. E.; Wellstein, A. Anti-apoptotic signaling of pleiotrophin through its receptor, anaplastic lymphoma kinase. *J. Biol. Chem.* **2002**, *277*, 35862–35868. (f) Powers, C.; Aigner, A.; Stoica, G. E.; McDonnell, K.; Wellstein, A. Pleiotrophin signaling through anaplastic lymphoma kinase is rate-limiting for glioblastoma growth. *J. Biol. Chem.* **2002**, *277*, 14153–14158. (g) Stoica, G. E.; Kuo, A.; Powers, C.; Bowden, E. T.; Sale, E. B.; Riegel, A. T.; Wellstein, A. Midkine binds to anaplastic lymphoma kinase (ALK) and acts as a growth factor for different cell types. *J. Biol. Chem.* **2002**, *277*, 35990–35998. (h) Lu, K. V.;

Jong, K. A.; Kim, G. Y.; Singh, J.; Dia, E. Q.; Yoshimoto, K.; Wang, Y.; Cloughesy, T. F.; Nelson, S. F.; Mischel, P. S. Differential induction of glioblastoma migration and growth by two different forms of pleiotrophin. *J. Biol. Chem.* **2005**, *280*, 26953−26964.

(24) Sauville, E. A.; Arbuck, S. G.; Messmann, R.; Headlee, D.; Bauer, K. S.; Lush, R. M.; Murgo, A.; Figg, W. D.; Lahusen, T.; Jaken, S.; Jing, X.; Roberge, M.; Fuse, E.; Kuwabara, T. Senderowicz, A. M. Phase I trial of 72-hour continuous infusion UCN-01 in patents with refractory neoplasms. *J. Clin. Oncol.* **2001**, *19*, 2319−2333.

(25) Bonvini, P.; Gastaldi, T.; Falini, B.; Rosolen, A. Nucleophosmin-Anaplastic Lymphoma Kinase (NPM-ALK), a novel hsp90-client tyrosine kinase: down-regulation of NPM-ALK expression and tyrosine phosphorylation in ALK+ CD30 lymphoma cells by the hsp90 antagonist 17-allylamino-17-demethoxygeldanamycin. *Cancer. Res.* **2002**, *62*, 1559−1566.

(26) Turturro, F.; Arnold, M. D.; Frist, A. Y.; Pulford, K. Model of inhibition of the NPM-ALK kinase activity by herbimycin A. *Clin. Cancer Res.* **2002**, *8*, 240−245.

(27) Anand, N. K.; Blazey, C. M.; Bowles, O. J.; Bussenius, J.; Costanzo, S.; Curtis, J. K.; Dubenko, L.; Kennedy, A. R.; Khoury, R. G.; Kim, A. I.; Mandlo, J. L.; Peto, C. J.; Rice, K. D.; Tsang, T. H. (Exelixis, Inc. USA). Preparation of pyrazolo[3,4-c]isoquinoline derivatives as anaplastic lymphoma kinase modulators. PCT int. Appl. 2005, WO 2005009389.

(28) Gunby, R. H.; Tartari, C. J.; Porchia, F.; Donella-Deana, A.; Scapozza, L.; Gambacorti-Passerini, C. An enzyme-linked immunosorbent assay to screen for inhibitors of the oncogenic anaplastic lymphoma kinase. *Haematologica* **2005**, *90*, 988−990.

(29) Manning, G.; Whyte, D. B.; Martinez, R.; Hunter, T.; Sudarsanam, S. The protein kinase complement of the human genome. *Science* **2002**, *298*, 1912−1934.

(30) Webb, T. R.; Lvovskiy, D.; Heinrich, M. C.; Yee, J. W. H. Discovery of novel inhibitors of tyrosine kinases. Presented at the 221st American Chemical Society National Meeting, San Diego, CA, April 1−5, 2001; ACS: Washington, DC.; MEDI-228.

(31) Toledo, L. M.; Lydon, N. B.; Elbaum, D. The structure-based design of ATP-site directed protein kinase inhibitors. *Curr. Med. Chem.* **1999**, *6*, 775−805.

(32) Levitzki, A. Protein Tyrosine kinase inhibitors as novel therapeutic agents. *Pharmacol. Ther.* **1999**, *82*, 231−239.

(33) Traxler, P.; Bold, G.; Buchdunger, E.; Caravatti, G.; Furet, P.; Manley, P.; O'Reilly, T.; Wood, J.; Zimmermann, J. Tyrosine kinase inhibitors: From rational design to clinical trials. *Med. Res. Rev.* **2001**, *21*, 499−512.

(34) Webb, T. R.; Melman, N.; Lvovskiy, D.; Ji, X.; Jacobson, K. A. The Utilization of a Unified Pharmacophore Query in the Discovery of New Antagonists of the Adenosine Receptor Family. *Bioorg. Med. Chem. Lett.* **2000**, *10*, 31−34.

(35) Lipinski, C. A.; Lombardo, F.; Dominy, B. W.; Feeney, P. J. Experimental and computational approaches to estimate solubility and permeability in drug discovery and development settings. *Adv. Drug Delivery Rev.* **2001**, *46*, 3−26.

(36) Hubbard, S. R. Crystal structure of the activated insulin receptor tyrosine kinase in complex with peptide substrate and ATP analog. *EMBO J.* **1997**, *16*, 5572−5581.

(37) Cardozo, T.; Totrov, M.; Abagyan, R. Homology modeling by the ICM method. *Proteins.* **1995**, *23*, 403−14.

(38) Mazur, A. K.; Abagyan, R. A. New methodology for computer-aided modelling of biomolecular structure and dynamics. 1. non-cyclic structures. *J. Biomol. Struct. Dyn.* **1989**, *6*, 815−832.

(39) Abagyan, R.; Argos, P. Optimal protocol and trajectory visualization for conformational searches of peptides and proteins *J. Mol. Biol.* **1992**, *225*, 519−532.

(40) Abagyan, R.; Totrov, M.; Kuznetsov, D. ICM: A new method for protein modeling and design: applications to docking and structure prediction from the distorted native conformation *J. Comput. Chem.* **1994**, *15*, 488−506.

(41) Totrov, M.; Abagyan, R., Eds. *Protein−ligand Docking as an Energy Optimization Problem. The thermodynamics of receptor-inhibitor interactions;* Raffa, R. B., Ed.; Wiley and Sons: New York, 2000.

(42) Schapira M.; Abagyan R.; Totrov, M. Nuclear hormone receptor targeted virtual screening. *J. Med. Chem.* **2003**, *46*, 3045−3059.

(43) Zhu, T.; Yan, Z.; Li, R. Unpublished results.

(44) Li, W.; Favelyukis, S.; Yang, J.; Zeng, Y.; Yu, J.; Gangjee, A.; Miller, W. T. Inhibition of insulin-like growth factor I receptor autophosphorylation by novel 6−5 ring-fused compounds. *Biochem. Pharmacol.* **2004**, *68*, 145−154.

(45) Furet, P.; Caravatti, G.; Lydon, N.; Priestle, J. P.; Sowadski, J. M.; Trinks, U.; Traxler, P. Modelling study of protein kinase inhibitors: binding mode of staurosporine and origin of the selectivity of CGP 52411. *J. Comput.-Aided Mol. Des.* **1995**, *9*, 465−472.

(46) Traxler, P.; Furet, P. Strategies toward the design of novel and selective protein tyrosine kinase inhibitors. *Pharmacol. Ther.* **1999**, *82*, 195−206.